Modulation of physicochemical and antioxidant properties of Pickering emulsions using colloidal lignin particles based on kraft softwood and hardwood acetone fractions

Giovana Colucci [a,b,c,d], Matteo Gigli [e,*], Massimo Sgarzi [e], Alírio E. Rodrigues [c,d], Claudia Crestini [e,*], M. Filomena Barreiro [a,b,*]

[a] Centro de Investigação de Montanha (CIMO), Instituto Politécnico de Bragança, Campus de Santa Apolónia, 5300-253 Bragança, Portugal
[b] Laboratório Associado para a Sustentabilidade e Tecnologia em Regiões de Montanha (SusTEC), Instituto Politécnico de Bragança, Campus de Santa Apolónia, 5300-253 Bragança, Portugal
[c] LSRE-LCM – Laboratory of Separation and Reaction Engineering - Laboratory of Catalysis and Materials, Faculty of Engineering, University of Porto, Rua Dr. Roberto Frias, 4200-465 Porto, Portugal
[d] ALiCE – Associate Laboratory in Chemical Engineering, Faculty of Engineering, University of Porto, Rua Dr. Roberto Frias, 4200-465 Porto, Portugal
[e] Department of Molecular Sciences and Nanosystems, Ca' Foscari University of Venice, Via Torino 155, 30172 Venezia Mestre, Italy

ARTICLE INFO

ABSTRACT

Colloidal lignin particles (CLPs) emerge as a sustainable alternative to traditional, fossil-based emulsion stabilizers. However, effectively outperforming the conventional ingredients requires addressing the challenges posed by lignin heterogeneity and structural complexity. In this study, one-step acetone fractionation was applied to softwood and hardwood kraft lignins to tackle the issue. The resulting soluble (AS) and insoluble (AI) fractions, along with the pristine lignins, underwent thorough characterization and were used to create CLPs through the hydrotropic precipitation. The acetone fraction-derived CLPs were tested for the first time as Pickering stabilizers. Notably, a strong correlation emerged between the structural traits of each lignin sample and the properties of the resulting Pickering emulsions. Such correlation allowed for a fine-tuning of their physicochemical and antioxidant features. The AS fractions, characterized by higher phenolic OH content and lower molecular weight, led to CLPs with larger sizes and reduced hydrophilic character compared to those derived from AI- and pristine lignins. The fraction-derived CLPs exhibited superior emulsifying capacity and imparted long-term stability to the formed emulsions. Moreover, the resulting Pickering emulsions showed high potential as antioxidant agents, proving their ability as multifunctional systems. Overall, this work demonstrates how the unique properties of lignin can be selectively enhanced through acetone fractionation method and seamlessly transferred to Pickering emulsions. This advancement promotes the use of lignin in high-value-added sectors such as cosmetics and personal care.

1. Introduction

Lignin is a natural and renewable polymer sourced primarily from plant cell walls. The abundance of aromatic compounds in lignin renders it a favorable candidate for substituting fossil-derived materials and traditional polymers [1]. Annually, millions of tons of technical lignins are available as by-products of industrial processes such as pulp and paper, biorefinery saccharification, and agri-food transformations [2,3]. However, less than 5 % of technical lignins are directed to added-value applications rather than to energy recovery [4,5]. The major drawback to lignin valorization lies in its complex chemical structure and variability. For example, during the kraft pulping process, the native lignin structure undergoes several modifications, including chemical fragmentation and recondensation [6]. The final kraft lignin is characterized by high heterogeneity in terms of molecular weight distribution and interunit bonding patterns, which vary according to the type and severity of the pulping process [3,7]. Despite these issues, technical lignins present remarkable functional properties such as antioxidant, UV

---

shielding ability, amphiphilic nature, biocompatibility, and eco-friendly connotation [8]. The need to overcome the dependence on fossil-based resources prompted extensive efforts toward the valorization of lignins. From this perspective, the development of colloidal lignin particles (CLPs) as Pickering stabilizers [8–11] is a rapidly emerging field. Pickering emulsions display enhanced stability and longer shelf-life than conventional surfactant-based emulsions due to the adsorption of solid particles at the oil–water interface, which acts as a physical barrier preventing coalescence effects [12]. Notably, the surfactant-free nature of Pickering emulsions confers biocompatibility, thus enabling their application in bio-based formulations in the cosmetic, personal care, and pharmaceutical industries [13,14].

Although CLPs have proven high potential as Pickering stabilizers, their emulsifying performance is significantly affected by lignin heterogeneity. As an example, kraft CLPs stabilized oil-in-water Pickering emulsions with different vegetal oils [8]. Such emulsions revealed high stability and the potential to be applied as UV protector boosters in cosmetic formulations, although the size and origin of CLPs influenced the emulsification process and the UV protection performance. In another study [10], CLPs were found to stabilize high-internal phase Pickering emulsions with enhanced UV shielding ability. The emulsion systems, consisting of different lignin preparations from eucalyptus, could protect curcumin, a hydrophobic drug model. However, the drug loading efficiency and UV shielding ability highly depended on the lignin extraction process and its properties, such as molecular weight and hydroxyl content.

Therefore, consistent quality and reproducibility in terms of chemical structure and performance clearly emerge as essential prerequisites for lignin use as a viable material for valuable applications, enabling it to effectively compete with fossil-based products [15]. Lignin fractionation techniques, including extraction with solvents, membrane ultrafiltration, and pH-dependent precipitation [15,16] have been proposed to tackle the challenges associated with its variability and diversity. Among them, one-step solvent fractionation has been proven a simple and economic solution, which successfully separates lignin into homogeneous and consistent cuts [3,17,18]. Argyropoulos *et al.* [1] demonstrated that acetone can be applied to obtain homogeneous and comparable kraft lignin fractions in terms of molecular weight and hydroxyl groups content regardless of the lignin source and pulping extraction severity [1,3]. In the case of kraft lignins, acetone fractionation is now widely reported in the literature [1,7,16,18–22]. Additionally, acetone is a non-toxic solvent and it is thus preferred in terms of economic assessment and environmental impact [20].

In this work, CLPs from acetone lignin fractions were explored for the first time in the stabilization of Pickering emulsions. With the purpose of achieving precise control over the functional properties of the prepared Pickering emulsions, a hardwood and a softwood kraft lignin were selected, subjected to acetone fractionation to obtain the respective acetone soluble (AS) and acetone insoluble (AI) cuts, and fully characterized to identify their specific chemical and structural features. Subsequently, CLPs were prepared by the hydrotropic precipitation, and their physicochemical properties (size, zeta potential, wettability, and morphology) were determined and correlated to the chemical structure of the CLPs-forming lignin. Then, the influence of the acetone fraction-derived CLPs on the stabilization and antioxidant capacity of Pickering emulsions was thoroughly interpreted.

2. Experimental

2.1. Materials

Ecolig, kindly supplied by Suzano (Brazil), is a hardwood kraft lignin from eucalyptus. Indulin AT, kindly supplied by Ingevity™ (USA), is a purified form of kraft softwood pine lignin (purity 97 %). Acetone, methanol, dimethyl sulfoxide (DMSO), 2-chloro-4,4,5,5-tetramethyl-1,3,2-dioxaphospholane (TMDP), deuterochloroform (CDCl₃), pyridine (anhydrous, 99.8 %), chromium (III) acetylacetonate (99.99 %), cholesterol, 2,2-diphenyl-1-picrylhydrazyl (DPPH), and 6-hydroxy-2,5,7,8-tetramethylchroman-2-carboxylic acid (Trolox) were purchased from Sigma-Aldrich (USA). Tungsten(VI)-oxide powder was purchased from Elementar Analysensysteme GmbH (Germany). Dimethyl sulfoxide ChromAR HPLC was purchased from Macron Fine Chemicals (USA). Sodium *p*-toluenesulfonate (Na-PTS) was purchased from TCI (Japan). Miglyol 812 was purchased from Acofarma (Spain). All chemicals were used without any further purification unless otherwise specified.

2.2. One-step acetone fractionation of kraft lignins

The pristine lignin powders (15 g), namely the softwood kraft lignin (SKL) and the hardwood kraft lignin (HKL), were mixed with acetone (500 mL) and left under stirring (500 rpm) overnight at room temperature. The acetone soluble (AS) and insoluble (AI) fractions were separated by filtration using Whatman paper filters under vacuum. The solvent from the AS fractions was removed in a rotary evaporator at 40 °C and reduced pressure (IKA RV10 and HB10, Germany). The AS and AI fractions were left to dry in a vacuum oven at 40 °C until constant weight. The solubility yields were gravimetrically calculated. The fractions were recovered and stored at room temperature prior to further analysis. Herein, the AS and AI fractions from SKL are designated AS-SKL and AI-SKL, respectively, while the AS and AI fractions from HKL are designated AS-HKL and AI-HKL, respectively.

2.3. Characterization of pristine lignins, AS, and AI fractions

2.3.1. Elemental analysis and ash determination

The pristine lignins' carbon, hydrogen, nitrogen, and sulfur contents were evaluated through CHNS analysis employing a UNICUBE instrument (Elementar, Germany). The ash content of the dried lignin samples was determined following the Tappi method T211 om-12, after calcination of the samples in a Thermolyne F6000 (Thermo Fisher Scientific, USA) furnace at 525 °C for 5 h.

2.3.2. Molecular weight (MW) distribution

MW distributions were obtained by gel permeation chromatography. Lignin samples were dissolved in HPLC-grade DMSO (0.2 g/L) and filtered through a 0.2 μm PTFE filter before injection. A Shimadzu instrument (Japan) consisting of a controller unit (CBM-20A), a pumping unit (LC 20AT), a degasser (DGU-20A3), a column oven (CTO-20AC), a diode array detector (SPD-M20A), and a refractive index detector (RID-10A) was used. The system was controlled by Shimadzu LabSolutions (Version 5.42 SP3) software. A PLgel 5 μm MiniMIX-C column was employed for the measurements. HPLC-grade DMSO containing 0.1 % LiCl was used as eluent (0.2 mL/min, 70 °C, elution time 25 min). Standard calibration was performed with polystyrene sulfonate standards (Sigma Aldrich, 4.3–2600 kDa) and lignin model compounds (330–640 Da).

2.3.3. Hydroxyl groups content

Hydroxyl groups content was determined by quantitative ³¹P NMR according to a reported procedure [23]. A precisely weighted amount of lignin sample (~30 mg) was solubilized in 500 μL of pyridine/CDCl₃ (1.6:1.0, v/v). After solubilization, 100 μL of the internal standard solution, i.e., cholesterol solution, was added. Finally, 100 μL of the phosphitylating reagent TMDP was added, and the mixture was vigorously shaken, transferred into an NMR tube, and immediately subjected to ³¹P NMR analysis. The spectra were recorded on a Bruker 400 MHz NMR (USA). All the reported chemical shifts are relative to the peak for the reaction product of water with TMDP (132.2 ppm). Data were processed with MestreNova (version 8.1.1, Mestrelab Research).

2.3.4. Color

The color was measured using a colorimeter CR-400 (Konica Minolta, Japan), where the L*, a*, and b* (CIELAB space) color parameters were determined. L* indicates the luminosity that goes from dark (0) to light (100), a* the green-red component that goes from green (−60) to red (60), and b* the blue-yellow component that goes from blue (−60) to yellow (60).

2.4. Production of CLPs and Pickering emulsions

CLPs were produced by the hydrotropic precipitation method, according to a procedure described previously [24], with minor modifications. Briefly, the lignin samples were dissolved into a Na-PTS 2 M aqueous solution (20 g/L). The mixture was placed in an ultrasound bath to ensure maximum solubilization. The solution was filtered using Whatman paper filters under vacuum. The clear solutions exhibiting different pH values (varying from 4.1 to 5.1) were acidified to pH 4 with HCl 0.1 M and then diluted by rapid water addition to achieve a final concentration of Na-PTS equal to 0.5 M. The formed CLPs were centrifuged (5810 R Centrifuge, Eppendorf, Germany) at 8014 g for 30 min and the solid was repeatedly washed until all the residual Na-PTS was removed. Finally, the particles were concentrated to 30 g/L by water evaporation using the rotary evaporator at 60 °C and reduced pressure. The CLPs yield was gravimetrically calculated after freeze-drying the samples at −105 °C in a Scanvac CoolSafe (LaboGene, Denmark).

Pickering emulsions were produced with the CLPs from pristine lignins and their acetone fractions according to a procedure described previously [14], with minor modifications. Equal volumes of each CLPs dispersion (30 g/L) and Miglyol 812 oil were used. The oil was added dropwise to the CLPs dispersion with continuous stirring at 13500 rpm using a CAT Unidrive X 1000 homogenizer (Germany). After completing the oil addition, the emulsion was further homogenized for 5 min. The emulsions were stored at room temperature.

2.5. Characterization of CLPs and Pickering emulsions

2.5.1. Size

The size of the CLPs and Pickering emulsion droplets (emulsified phase) were measured by laser diffraction analysis using a Mastersizer 3000 equipped with a Hydro MV dispersion unit (Malvern Instruments Ltd., United Kingdom). The refractive index and absorption were set to 1.6 and 0.1, respectively, following published data [25,26].

2.5.2. Zeta potential

The zeta potential of CLPs was determined by particle electrophoresis using a Nano-ZS Zetasizer instrument (Malvern Instruments Ltd., United Kingdom) equipped with a standard DTS1070 disposable folded capillary cell.

2.5.3. Wettability

The air–water contact angle of the CLPs was measured on a Goniometer (model 210, Ramé-hart Instrument Co., USA). CLPs were freeze-dried, and pellets with a diameter of 13 mm and a thickness of about 2 mm were prepared using a hydraulic press (Specac Ltd., United Kingdom) at 10 tonnes for 2 min. The pellets' surface was previously checked by optical microscopy (Nikon Eclipse 50i, Nikon Corporation, Japan) to discard those with surface cracks. The water contact angle was determined using the sessile drop method at room temperature 10 s after the deposition of the water droplet (5 μL).

2.5.4. Morphology

CLPs morphology was assessed with a scanning electron microscope (SEM) JEOL JSM-5600LV (Japan) after sputtering samples with gold. Emulsion morphology was evaluated by optical microscopy using a Nikon Eclipse 50i (Nikon Corporation, Japan) equipped with Nikon Digital. Sample aliquots (emulsified phase) were placed on a microscope slide and gently covered with a coverslip. Image acquisition and processing were performed using NIS-Elements Documentation software after 1 day of storage.

2.5.5. Emulsified layer (EL)

The EL of the Pickering emulsions was calculated according to Eq. (1) [27]:

$$EL(\%) = H_E \times 100/H_T \tag{1}$$

where H_E is the height of the emulsion layer and H_T is the total sample height.

2.5.6. Antioxidant activity

The antioxidant activity was analyzed through the DPPH radical scavenging analysis, following a previously described procedure [28], with minor modifications. DMSO was used as the solvent for the lignin samples and Pickering emulsions and water was used for CLPs to dilute the samples at different lignin concentrations (0.05 to 4000 μg/mL). For the assay, 270 μL of DPPH methanolic solution (6×10^{-5} mol/L) was added to 30 μL of each sample. After 30 min in the dark at room temperature, the inhibition of the DPPH radical was measured at a wavelength of 517 nm in a microplate spectrophotometer (Epoch, Agilent, USA). Trolox was used as a positive control. The inhibition percentage of the DPPH radical was calculated according to Eq. (2).

$$DPPH\ Inhibition(\%) = (A_{control} - A_{sample}) \times 100/A_{control} \tag{2}$$

where A_{sample} is the absorbance of DPPH with the lignin sample, and $A_{control}$ is the absorbance of DPPH without lignin. The radical scavenging ability of the tested samples was expressed as the half-maximal inhibitory concentration (IC_{50}).

3. Results and discussion

3.1. Characterization of pristine lignins, AS, and AI fractions

In this work, a softwood kraft lignin (SKL) from pine and a hardwood kraft lignin (HKL) from eucalyptus were subjected to acetone fractionation, resulting in acetone soluble (AS-SKL and AS-HKL) and acetone insoluble (AI-SKL and AI-HKL) cuts. The HKL revealed a high solubility yield (71 ± 5 %), whereas the SKL was poorly dissolved in acetone (27 ± 7 %). Elemental analysis and ash content were determined to elucidate lignin composition (Table S1). Both lignins presented similar carbon, oxygen, and hydrogen contents, comparable with values from the literature for kraft lignins [18,22,29]. The HKL presented higher sulfur and ash contents (2.34 ± 0.06 % and 4.17 ± 0.06 %, respectively) than the SKL (1.66 ± 0.02 % and 3.26 ± 0.03 %, respectively). The increase of inorganics in lignin composition decreases its solubility in organic solvents [21]. Nevertheless, this correlation was not evident in this work, suggesting that other lignin structural characteristics played a role in the fractionation process.

It was previously stated that the lignin solubility in a given solvent is highly related to its functional groups and MW [30]. Table 1 summarizes the weight-average MW (M_w) and the dispersity index (Đ) and Table 2 lists the hydroxyl (OH) groups of the lignin samples. MW distributions and ^{31}P NMR spectra can be seen in Fig. S1. The HKL had a lower MW and Đ compared to the SKL. The higher MW of SKL *versus* HKL is due to the low severity index of the indulin process (SKL) used for pine instead of the kraft process that yielded the HKL. The milder conditions adopted in the indulin process, as a matter of fact, determines the retention of higher MW lignin fragments. In addition, the larger Đ observed for SKL is reasonably caused by the higher degree of branching of this lignin with respect to HKL, due to the prevalence of G units (Table 2) that can form further bonding motifs on the C5 position [7]. Moreover, although SKL and HKL had a similar content of total phenolic and carboxyl OH groups, SKL presented a higher aliphatic OH content than HKL. The

Table 1

Molecular weights and L*, a*, and b* color parameters of the softwood (SKL) and hardwood (HKL) pristine kraft lignins and their acetone soluble (AS) and insoluble (AI) fractions.

	M_w	Đ	L*	a*	b*	RGB color
SKL	10400	5.6	42.05 ± 0.04	7.91 ± 0.03	10.42 ± 0.04	
AS-SKL	2000	2.1	58.6 ± 0.4	7.11 ± 0.07	23.3 ± 0.2	
AI-SKL	14900	4.1	52.81 ± 0.08	5.83 ± 0.01	16.32 ± 0.04	
HKL	5100	3.4	37.94 ± 0.07	4.76 ± 0.06	3.94 ± 0.06	
AS-HKL	2900	2.3	43.05 ± 0.02	5.39 ± 0.02	8.7 ± 0.1	
AI-HKL	16700	3.0	42.0 ± 0.1	4.17 ± 0.04	6.50 ± 0.02	
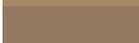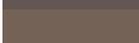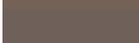
M_w: weight-average molecular weight, Đ: dispersity index.

Table 2

Hydroxyl groups content (mmol/g) of the softwood (SKL) and hardwood (HKL) pristine kraft lignins and their acetone soluble (AS) and insoluble (AI) fractions.

Functional group	SKL	AS-SKL	AI-SKL	HKL	AS-HKL	AI-HKL
Aliphatic OH	2.41	1.67	2.57	0.96	0.86	1.20
Syringyl OH	0.16	0.18	0.14	1.21	1.40	0.58
4-O-5′ OH	0.41	0.43	0.37	1.23	1.36	0.84
5-5′ phenolic OH	0.71	0.74	0.69	0.28	0.29	0.27
Total Cond. OH	1.60	1.76	1.44	2.81	3.13	1.80
Guaiacyl OH	1.72	2.60	1.21	0.74	0.81	0.48
p-Hydroxyphenyl OH	0.32	0.34	0.28	0.17	0.17	0.14
Total Non-Cond. OH	2.05	2.94	1.49	0.91	0.98	0.61
Total phenolic OH	3.65	4.70	2.93	3.72	4.11	2.41
Carboxyl OH	0.42	0.59	0.29	0.47	0.48	0.32
Total OH*	6.48	6.96	5.79	5.14	5.45	3.94

* Sum of Aliphatic OH, Total phenolic OH, and Carboxyl OH contents. Repeated measurements highlighted differences not larger than 0.02 mmol/g.

observed differences in MW and structural characteristics explain the lower fractionation yield observed for SKL in comparison to HKL, which, on the contrary, displayed higher solubility in acetone.

As expected from the acetone treatment, the acetone fractions presented higher homogeneity (lower Đ) than the corresponding pristine lignins, and the AS fractions were characterized by a lower MW than the AI ones [15,22,30]. Furthermore, the AS fractions presented a significantly higher content of total phenolic OH, whereas the AI fractions showed the opposite trend, with a higher content of aliphatic OH. These results agree with the reported literature on acetone lignin fractionation [1,3,20,22]. In summary, AS fractions, corresponding to the low MW fragments of the pristine lignin, are highly branched and show a high content of phenolic OH groups formed during the kraft pulping process due to depolymerization and repolymerization reactions. In contrast, AI fractions consist of high MW lignin fragments, showing a structure characterized by longer chains with aliphatic residues, which is more similar to native lignin [3].

Significant color variations were observed among the lignin samples (Table 1), also reflecting differences in the chemical structure and aggregation state. HKL presented a darker brown color (lower L*, a*, and b* values) than SKL presumably due to the harsher pulping process used in the case of HKL. Furthermore, the AS and AI fractions were lighter (higher L* values) than their corresponding pristine lignins. The tendency for red (+a*) was similar among samples, however, a pronounced propensity for yellow (+b*) was observed for the acetone fractions when compared to the pristine lignins. The lignin color has been attributed to chromophores formed during kraft pulping, including carbonyl functional groups, conjugated phenolics, quinoid structures, and metal complexes [31]. However, the obtained results cannot be explained

based on the prevalent presence of condensed or chromophoric structures in specific lignin fractions. In fact, in this case, the darker fractions were the high MW ones that typically contain a lower amount of condensed and conjugated subunits than the low MW ones. The aggregation morphology of the lignin samples after drying is, from this perspective, a pivotal factor. The studies conducted by Zhang *et al.* [32,33] showed that a low bulk density decreases the chromophore concentration at the macroscopic level, resulting in lighter brown hues of lignin when in a solid state. Indeed, for both lignin types, the AS fraction that was dissolved in acetone and that underwent solvent evaporation was lighter than the AI fractions. However, the relationship between the aggregation processes, morphology, and chemical structure requires further investigation.

3.2. Effect of fractionation on CLPs properties

CLPs were produced with the pristine lignin samples and their respective AS and AI fractions using the hydrotropic precipitation technique. It consists of the lignin solubilization in an aqueous solution of the hydrotrope *p*-toluene sulfonate (Na-PTS), a non-toxic organic salt, followed by the addition of the antisolvent water to decrease lignin solubility in the medium and, thus, cause the particles' precipitation. Afterward, the particles are centrifuged and washed to remove the hydrotrope completely, which can be recycled several times in the process [24]. By this strategy, particle formation follows similar principles to those of antisolvent precipitation techniques, yet it is reported as more efficient in terms of particle formation, and it can be applied to different lignins without the need for specific adjustments [24].

Fig. 1a shows the visual aspect of the CLPs, and Table S2 and Fig. S2 show the yield and particle size distributions, respectively. Regarding the CLPs size (Fig. 1b), for both lignin types, the particles from the AS fractions had larger sizes than those from the corresponding pristine lignin, followed by those from the AI fractions. This behavior is consistent with previous studies [5,30,34–36], and it is directly related to the MW and chemical composition of each lignin sample. It is well reported that during the CLPs formation, the lignin hydrophobic groups constitute the core, whereas the more hydrophilic groups are located at the CLPs surface [36]. Therefore, the AI lignin fractions, which are characterized by a higher MW and a lower content of total OH groups (Table 2), readily aggregate forming a core structure upon water addition, resulting in compact nuclei particles. In contrast, the AS lignin fractions, characterized by a lower MW and a higher content of total OH groups, strongly interact with water molecules, thus requiring additional lignin chains to facilitate self-assembly [17]. This leads to the formation of larger CLPs, where the growth of particles is favored over nucleation [36]. For the pristine lignin samples, the high MW fragments first nucleate, followed by the adsorption of the low MW fragments at
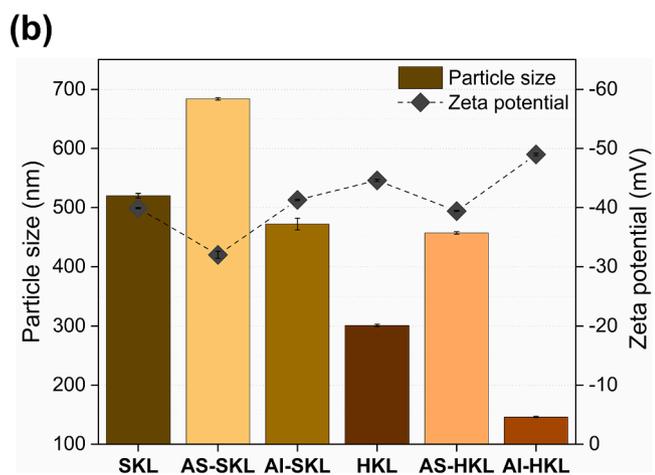
Fig. 1. (a) Visual aspect of colloidal lignin particles produced from the softwood (SKL) and hardwood (HKL) pristine kraft lignins and their acetone soluble (AS) and insoluble (AI) fractions; (b) average particle size and zeta potential.

the CLPs surface, yielding intermediate sizes compared to the acetone fractions. Noteworthy is that this correlation is only applicable to the comparison between fractions from the same lignin.

When comparing the distinct lignin types, the CLPs from the hardwood-type samples presented smaller sizes (146–457 nm) than those from the softwood-type samples (472–684 nm). In fact, previous studies [34,37] pointed out that a direct relationship between MW and particle size could not be made when comparing samples from distinct lignin types and extraction processes, suggesting that additional structural factors play a significant role in particle size. It can be hypothesized that the different degree of branching between the two lignins affects the formation of CLPs. As above mentioned, the structure of softwood lignin, mainly composed of G units, is more branched and thus less densely packed, resulting in larger CLPs [38]. Furthermore, the softwood-type samples presented a higher total OH content (Table 2) than the hardwood-type samples, suggesting that the former are more hydrophilic, thus yielding larger particles [39]. Regarding the CLPs morphology (Fig. S3), all CLPs exhibited spherical shapes and smooth surfaces, with no significant differences between samples.

To further elucidate the obtained results, the wettability of CLPs was analyzed (Fig. 2). For both lignin types, CLPs from the AS fractions exhibited a less hydrophilic character compared to the CLPs from the AI fractions and the pristine lignins, suggesting relevant differences in the conformation and exposure of functional groups on the particles' surface. Yang et al. [40] observed that the phenolic OH and carboxyl OH groups content significantly decreased in CLPs when compared to the initial lignin. In this sense, it is very likely that the low MW fragments of the AS fractions, being the most hydrophilic ones, did not participate in CLPs formation, thus remaining in solution. Therefore, the surface of CLPs from AS fractions presented fewer hydrophilic groups than
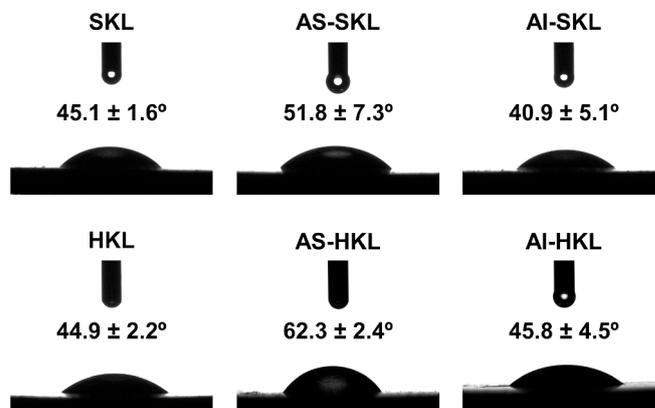

Fig. 2. Air-water contact angles of colloidal lignin particles produced from the softwood (SKL) and hardwood (HKL) pristine kraft lignins and their acetone soluble (AS) and insoluble (AI) fractions.

expected. On the other hand, the high MW fragments contained in the AI fractions and pristine lignins formed hydrophobic small nuclei followed by the adsorption of small polar lignin fragments on the CLPs surface [35]; thus, these CLPs exhibit a more hydrophilic character. The same behavior was reported by Tian et al. [41], in which CLPs produced from the THF-soluble fraction presented a less hydrophilic character, despite the initial lignin fraction having the highest content of total OH groups. This suggests that the wettability of CLPs cannot be directly correlated with OH groups content. Furthermore, the preparation of CLPs by the hydrotropic approach might have an influence on the wettability differences since hydrophobic interactions between the lignin aromatic structures and Na-PTS take place, which would result in a different organization of the OH groups on the formed CLPs [24].

The zeta potential of CLPs is shown in Fig. 1b. As expected, all CLPs presented a negative charge on their surface due to the presence of the OH groups [5]. The same trend was obtained for both lignin types, i.e., the CLPs from the AI fractions were more negatively charged than the ones from the corresponding pristine lignin samples, followed by the CLPs from the AS fractions. This well agrees with the wettability results, as the more hydrophilic CLPs have a more negatively charged surface (AI fractions), whereas the less hydrophilic CLPs present the less negative charge values (AS fractions). Moreover, the data highlight that the higher the charge density, the smaller the particle size, as previously observed by Pylypchuk et al. [42] in hardwood and softwood kraft nanoparticles.

3.3. Effect of fractionation on Pickering emulsions stabilization

To investigate the formation and stabilization of Pickering emulsions with CLPs from the different lignin samples (pristine lignins and their acetone fractions), the emulsions were produced with the same CLPs concentration (30 g/L) and an oil volume fraction of 0.5, a usual approach to preliminary analyze emulsion formation and stabilizing capability of the particles [27,41,43–45]. As expected, all emulsions were oil-in-water type due to the hydrophilic character of CLPs (Fig. 2) [12].

The emulsions exhibited a bimodal droplet size distribution (Fig. S4) and the volume-average diameter $d_{4,3}$ was chosen to represent the overall size distribution (Fig. 3a). One relevant factor influencing the droplet size of Pickering emulsions is the size of the stabilizing particles, where the larger the particle size the larger the droplets formed during emulsification, due to longer particle adsorption times at the oil–water interface [12]. However, in this work, a direct correlation between particle and droplet sizes was not observed. For example, pristine and AI CLPs had distinct particle sizes (Fig. 1b) although stabilized emulsions with similar droplet sizes (between 13 and 17 μm). In fact, the particle
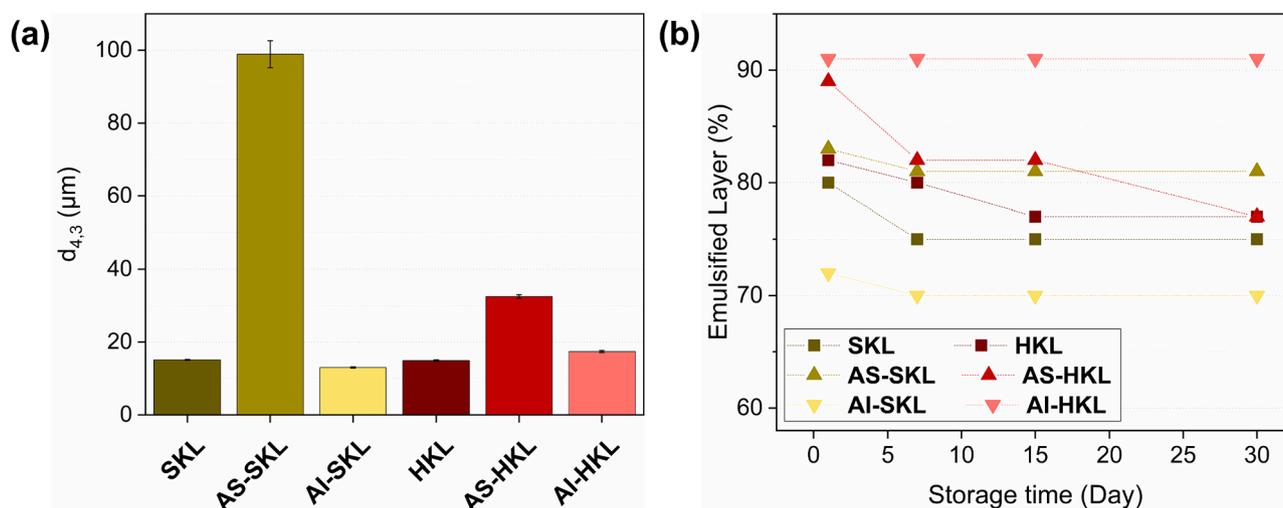
Fig. 3. Characterization of Pickering emulsions produced with colloidal lignin particles from the softwood (SKL) and hardwood (HKL) pristine kraft lignins and their acetone soluble (AS) and insoluble (AI) fractions: (a) volume-average droplet size $d_{4,3}$ and (b) emulsified layer.

wettability is reported to influence the droplet size, where particles having a more hydrophilic character are more surface active and tend to stabilize small oil droplets [41,46]. For the produced emulsions, it seems that the particle wettability was a more relevant factor influencing the droplet size, as the CLPs from pristine and AI fractions exhibited similar wettability values (Fig. 2) with a more hydrophilic character and stabilized emulsions with small droplets, whereas CLPs from the AS fractions exhibited a less hydrophilic character and stabilized larger droplets.

The Pickering stabilizing capacity of CLPs was assessed by measuring the formed emulsified layer (EL) expressed as a percentage relative to the total sample [27]. Thus, the higher the EL the better the emulsifying capacity. All the samples exhibited ELs equal to or higher than 70 % (Fig. 3b), maintaining this state during 30 days of storage, indicating that CLPs were strongly adsorbed at the oil–water interface and the emulsions presented excellent long-term stability. Interestingly, a trend between the EL and the droplet-to-particle size ratio was observed (Table S3). Namely, the higher the droplet-to-particle size ratio, the higher the EL. This agrees with the claim that particles should be substantially smaller than the emulsion droplets, at least of one order of

magnitude, to effectively adsorb at the oil–water interface, forming structured interface layers [47]. Indeed, a high droplet-to-particle ratio is recommended to increase adsorption energy, which is proportional to the contact area [48,49], resulting in higher emulsification performance.

Furthermore, it is worth noting that, for the used conditions, the emulsions prepared with the AI-HKL and AS-HKL CLPs showed a higher emulsifying ability than HKL (AI-HKL > AS-HKL > HKL); and for the softwood-type samples, the emulsifying capacity followed the order AS-SKL > SKL > AI-SKL. Thus, this result highlights that the fractionation improved the lignin emulsifying capacity.

The visual aspect and optical microscopy images of Pickering emulsions are displayed in Fig. 4. Emulsions from the hardwood-type samples exhibited a dark brown hue due to the darker color of the HKL and its acetone fractions when compared to the softwood-type samples, which had lighter brown hues. The microscopy images agreed with the droplet size results obtained by laser diffraction, revealing a high droplet concentration due to the high CLPs concentration and high emulsification energy used in the production, which creates a large total interfacial area and induces particle adsorption,
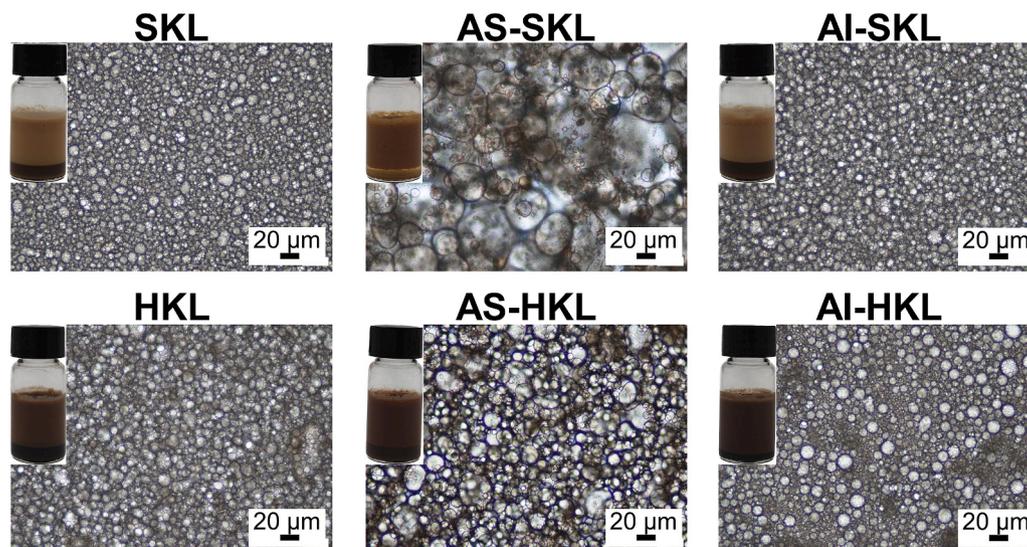
Fig. 4. Visual aspect and optical microscopy of Pickering emulsions produced with colloidal lignin particles from the softwood (SKL) and hardwood (HKL) kraft lignins and their acetone soluble and insoluble fractions (AS and AI).

yielding many oil droplets [12]. Regarding the emulsion morphology, it was observed that the emulsion produced with the SKL CLPs showed small droplets with irregular morphology. On the other hand, AS-SKL CLPs gave rise to round yet deformable large droplets, whereas the AI-SKL ones generated well-defined round droplets. The emulsions stabilized with the hardwood-type CLPs exhibited spherical droplets, with the one from AI-HKL revealing more defined and structured droplets. Since the AS-based Pickering emulsions exhibited larger droplet sizes, a lower interfacial area was formed, and a considerable amount of CLPs remained in excess in the aqueous phase. For this reason, it is possible to observe brown agglomerates in the corresponding microscopy images.

3.4. Effect of fractionation on antioxidant performance

The antioxidant activity of the pristine lignins and acetone fractions (initial lignins), the corresponding CLPs, and respective Pickering emulsions was evaluated through the DPPH radical scavenging methodology. Table 3 lists the IC_{50} values, representing the sample concentration required to inhibit 50 % of the DPPH free radical, i.e., the lower the IC_{50}, the higher the antioxidant capacity. The results highlighted that the initial lignins from the hardwood-type samples (HKL, AS-HKL, and AI-HKL) had higher antioxidant activity than the softwood-type samples (SKL, AS-SKL, and AI-SKL), suggesting that the lignin type influenced the results. The antioxidant activity is usually directly correlated with the total phenolic OH groups content [50]. However, this effect was not evident in this work since both lignin types presented similar values of total phenolic OH (Table 2), and a higher activity was observed for the hardwood-type samples. In fact, the antioxidant activity of lignin is attributed to the overall lignin structure and functionality, where a combination of high amount of phenolic OH groups, high amount of syringyl OH, and lower MW have a positive effect on the antioxidant properties [22,51,52]. On these bases, the higher antioxidant capacity of hardwood-type samples can be easily explained.

Considering the CLPs, a higher antioxidant activity (lower IC_{50}) was evidenced comparatively to the initial lignin samples. This behavior is commonly reported and attributed to the small size of CLPs and molecular rearrangement of lignin molecules, resulting in a high total surface area and better accessibility of the lignin functional groups to free radicals [53–55]. In addition, all CLPs exhibited IC_{50} values in the same magnitude order as Trolox, highlighting their potential to replace synthetic antioxidants.

When comparing the samples from the same lignin type, i.e., pristine lignin and acetone fractions, the antioxidant activity followed the order: AS fraction > pristine lignin > AI fraction, in the case of initial lignins and CLPs, in agreement with the obtained data on the total phenolic OH groups content and MW. However, this trend was not observed for the produced Pickering emulsions, suggesting that their antioxidant activity was likely influenced by the CLPs distribution in emulsion structure. Despite a slight increase, the IC_{50} values of the Pickering emulsions were very close to those of the corresponding CLPs, proving the ability of CLPs to act as radical scavengers even when distributed in the emulsion structure. The emulsions stabilized with the hardwood-type CLPs revealed very close IC_{50} values to the antioxidant Trolox (with only a difference of about 2, 3, and 5 μg/mL for HKL, AS-HKL, and AI-HKL, respectively), which reflects the inherent antioxidant activity of this lignin type. For the softwood-type emulsions, higher IC_{50} values were obtained, yet they also presented relatively close values to Trolox (with a difference of about 8, 9, and 11 μg/mL for SKL, AI-SKL, and AS-SKL). Thus, the overall results highlight the potential use of the produced Pickering emulsions as bio-based antioxidant systems.

4. Conclusions

One-step acetone fractionation of kraft lignin is a very simple, yet winning strategy to prepare highly stable and performant Pickering emulsions, whose final characteristics can be tuned based on the specific

Table 3
Antioxidant activity expressed as inhibitory concentration IC_{50} (μg/mL) of lignin samples.

	Initial lignin	CLPs	Pickering emulsions*
SKL	11.3 ± 1.4	6.2 ± 1.6	11.4 ± 1.7
AS-SKL	7.3 ± 3.3	4.3 ± 1.1	14.4 ± 3.4
AI-SKL	15.5 ± 1.4	9.4 ± 1.8	12.4 ± 1.1
HKL	3.9 ± 1.6	5.1 ± 0.7	5.1 ± 0.5
AS-HKL	3.3 ± 2.4	3.2 ± 0.6	6.1 ± 0.6
AI-HKL	10.0 ± 0.6	6.6 ± 0.6	8.6 ± 1.1
Trolox**	3.2 ± 0.2	–	–

* For the Pickering emulsions, the IC_{50} was calculated in function of colloidal lignin particles (CLPs) concentration.
** Positive control.

lignin type and cut employed as starting material for their preparation.

Indeed, the acetone fractionation successfully separated comparable and homogeneous fractions from the two kraft lignin sources, whose specific structural properties well correlated with the characteristics of the corresponding CLPs, in turn impacting the final properties of the Pickering emulsions. More specifically, the AI lignin fractions displayed relatively higher MW and aliphatic OH content, leading to CLPs with small size, more negative zeta potential, and a more hydrophilic surface. Conversely, AS lignin cuts presented low MW and high phenolic OH content, giving rise to CLPs with large size, less negative zeta potential, and a less hydrophilic surface. Overall, the fraction-derived CLPs resulted in improved emulsifying capacity when applied in the Pickering stabilization.

Notably, the experimental data showed for the first time that the high antioxidant activity of the lignin samples, clearly dependent on their chemical composition and structure, was not only transferred to the CLPs, yet nicely preserved also in the Pickering emulsions, these last presenting IC_{50} values comparable to the commercially available antioxidant molecule Trolox. In conclusion, the present study advances the full comprehension of the role played by distinct lignin fractions in stabilizing Pickering emulsions, thereby unlocking their applicability as a key multifunctional component of sustainable high-value-added products in diverse strategic fields such as pharmaceuticals, cosmetics, drug delivery, nutraceuticals, and fine chemical synthesis.

CRediT authorship contribution statement

Giovana Colucci: Writing – review & editing, Writing – original draft, Validation, Methodology, Investigation, Formal analysis, Conceptualization. **Matteo Gigli:** Writing – review & editing, Validation, Supervision, Resources, Methodology, Investigation, Conceptualization. **Massimo Sgarzi:** Writing – review & editing, Validation, Supervision, Methodology, Conceptualization. **Alírio E. Rodrigues:** Writing – review & editing, Supervision, Project administration. **Claudia Crestini:** Writing – review & editing, Supervision, Resources, Project administration, Funding acquisition, Conceptualization. **M. Filomena Barreiro:** Writing – review & editing, Supervision, Resources, Project administration, Funding acquisition, Conceptualization.

Declaration of competing interest

The authors declare that they have no known competing financial interests or personal relationships that could have appeared to influence the work reported in this paper.

Data availability

Data will be made available on request.

Acknowledgments

The authors are grateful to the Foundation for Science and Technology (FCT, Portugal) for financial support through national funds FCT/MCTES (PIDDAC) to CIMO UIDB/00690/2020 (DOI: 10.544 99/UIDB/00690/2020) and UIDP/00690/2020 (DOI: 10.544 99/UIDP/00690/2020); SusTEC LA/P/0007/2020 (DOI: 10.54499/ LA/P/0007/2020); LSRE-LCM UIDB/50020/2020 (DOI: 10.544 99/UIDB/50020/2020) and UIDP/50020/2020 (DOI: 10.544 99/UIDP/50020/2020); and ALiCE LA/P/0045/2020 (DOI: 10.54499/ LA/P/0045/2020). FCT for the Ph.D. research grant of G. Colucci (2021.05215.BD). Daniele Massari, Valeria Gagliardi, and Maryam RahimiHaghighi for the technical support and assistance to conduct experiments. Suzano for the kind supply of Ecolig lignin. Ingevity^{TM} for the kind supply of Indulin AT lignin. COST Action LignoCOST (CA17128), supported by COST (European Cooperation in Science and Technology), in promoting interaction, exchange of knowledge, and collaborations in the field of lignin valorization.

Appendix A. Supplementary data

Supplementary data to this article can be found online at https://doi. org/10.1016/j.seppur.2024.127570.

References

[1] D.S. Argyropoulos, H. Sadeghifar, C. Cui, S. Sen, Synthesis and characterization of poly(arylene ether sulfone) kraft lignin heat stable copolymers, ACS Sustain. Chem. Eng. 2 (2014) 264–271, https://doi.org/10.1021/sc4002998.

[2] L. Dessbesell, M. Paleologou, M. Leitch, R. Pulkki, C. (Charles) Xu, Global lignin supply overview and kraft lignin potential as an alternative for petroleum-based polymers, Renew. Sustain. Energy Rev. 123 (2020) 109768, https://doi.org/ 10.1016/j.rser.2020.109768.

[3] M. Gigli, C. Crestini, Fractionation of industrial lignins: opportunities and challenges, Green Chem. 22 (2020) 4722–4746, https://doi.org/10.1039/ d0gc01606c.

[4] B.D.S. Marotti, V. Arantes, Ultra-refining for the production of long-term highly pH-stable lignin nanoparticles in high yield with high uniformity, Green Chem. 24 (2022) 1238–1258, https://doi.org/10.1039/D1GC03525H.

[5] T. Pang, G. Wang, H. Sun, L. Wang, Q. Liu, W. Sui, A.M. Parvez, C. Si, Lignin fractionation for reduced heterogeneity in self-assembly nanosizing: toward targeted preparation of uniform lignin nanoparticles with small size, ACS Sustain. Chem. Eng. 8 (2020) 9174–9183, https://doi.org/10.1021/ acssuschemeng.0c02967.

[6] D.D.S. Argyropoulos, C. Crestini, C. Dahlstrand, E. Furusjö, C. Gioia, K. Jedvert, G. Henriksson, C. Hulteberg, M. Lawoko, C. Pierrou, J.S.M. Samec, E. Subbotina, H. Wallmo, M. Wimby, Kraft lignin: a valuable, sustainable resource, opportunities and challenges, ChemSusChem. 16 (2023) e202300492.

[7] C. Crestini, H. Lange, M. Sette, D.S. Argyropoulos, On the structure of softwood kraft lignin, Green Chem. 19 (2017) 4104–4121, https://doi.org/10.1039/ C7GC01812F.

[8] O. Gordobil, N. Blažević, M. Simonič, A. Sandak, Potential of lignin multifunctionality for a sustainable skincare: Impact of emulsification process parameters and oil-phase on the characteristics of O/W Pickering emulsions, Int. J. Biol. Macromol. 233 (2023) 123561, https://doi.org/10.1016/j. ijbiomac.2023.123561.

[9] J. Tomasich, S. Beisl, M. Harasek, Production and characterisation of pickering emulsions stabilised by colloidal lignin particles produced from various bulk lignins, Sustainability 15 (2023) 3693, https://doi.org/10.3390/su15043693.

[10] H. Zhang, F. Yue, S. Hu, H. Qi, F. Lu, Nanolignin-based high internal phase emulsions for efficient protection of curcumin against UV degradation, Int. J. Biol. Macromol. 228 (2023) 178–185, https://doi.org/10.1016/j.ijbiomac.2022.12.123.

[11] M. Yu, H. Xin, D. He, C. Zhu, Q. Li, X. Wang, J. Zhou, Electrospray lignin nanoparticles as Pickering emulsions stabilizers with antioxidant activity, UV barrier properties and biological safety, Int. J. Biol. Macromol. 238 (2023) 123938, https://doi.org/10.1016/j.ijbiomac.2023.123938.

[12] C. Albert, M. Beladjine, N. Tsapis, E. Fattal, F. Agnely, N. Huang, Pickering emulsions: preparation processes, key parameters governing their properties and potential for pharmaceutical applications, J. Control. Release. 309 (2019) 302–332, https://doi.org/10.1016/j.jconrel.2019.07.003.

[13] L. Ming, H. Wu, A. Liu, A. Naeem, Z. Dong, Q. Fan, G. Zhang, H. Liu, Z. Li, Evolution and critical roles of particle properties in Pickering emulsion: a review, J. Mol. Liq. 388 (2023) 122775, https://doi.org/10.1016/j.molliq.2023.122775.

[14] A. Sharkawy, M.F. Barreiro, A.E. Rodrigues, Preparation of chitosan/gum Arabic nanoparticles and their use as novel stabilizers in oil/water Pickering emulsions, Carbohydr. Polym. 224 (2019) 115190, https://doi.org/10.1016/j. carbpol.2019.115190.

[15] O. Gordobil, R.H. Diaz, J. Sandak, A. Sandak, One-step lignin refining process: the influence of the solvent nature on the properties and quality of fractions, Polymers (Basel) 14 (2022) 2363, https://doi.org/10.3390/polym14122363.

[16] C. Cui, R. Sun, D.S. Argyropoulos, Fractional precipitation of softwood kraft lignin: isolation of narrow fractions common to a variety of lignins, ACS Sustain. Chem. Eng. 2 (2014) 959–968, https://doi.org/10.1021/sc400545d.

[17] R. Liu, A. Smeds, T. Tirri, H. Zhang, S. Willför, C. Xu, Influence of carbohydrates covalently bonded with lignin on solvent fractionation, thermal properties, and nanoparticle formation of lignin, ACS Sustain. Chem. Eng. 10 (2022) 14588–14599, https://doi.org/10.1021/acssuschemeng.2c04498.

[18] M.A. Karaaslan, M. Cho, L.-Y. Liu, H. Wang, S. Renneckar, Refining the properties of softwood kraft lignin with acetone: effect of solvent fractionation on the thermomechanical behavior of electrospun fibers, ACS Sustain. Chem. Eng. 9 (2021) 458–470, https://doi.org/10.1021/acssuschemeng.0c07634.

[19] H. Gao, M. Sun, Y. Duan, Y. Cai, H. Dai, T. Xu, Controllable synthesis of lignin nanoparticles with antibacterial activity and analysis of its antibacterial mechanism, Int. J. Biol. Macromol. 246 (2023) 125596, https://doi.org/10.1016/j. ijbiomac.2023.125596.

[20] C.A.E. Costa, F.M. Casimiro, C. Vega-Aguilar, A.E. Rodrigues, Lignin valorization for added-value chemicals: kraft lignin versus lignin fractions, ChemEngineering. 7 (2023) 42, https://doi.org/10.3390/chemengineering7030042.

[21] M. Arefmanesh, S. Nikafshar, E.R. Master, M. Nejad, From acetone fractionation to lignin-based phenolic and polyurethane resins, Ind. Crops Prod. 178 (2022) 114604, https://doi.org/10.1016/j.indcrop.2022.114604.

[22] A. Tagami, C. Gioia, M. Lauberts, T. Budnyak, R. Moriana, M.E. Lindström, O. Sevastyanova, Solvent fractionation of softwood and hardwood kraft lignins for more efficient uses: compositional, structural, thermal, antioxidant and adsorption properties, Ind. Crops Prod. 129 (2019) 123–134, https://doi.org/10.1016/j. indcrop.2018.11.067.

[23] D.S. Argyropoulos, N. Pajer, C. Crestini, Quantitative 31P NMR analysis of lignins and tannins, J. vis. Exp. 174 (2021) e62696.

[24] S. Cailotto, M. Gigli, M. Bonini, F. Rigoni, C. Crestini, Sustainable strategies in the synthesis of lignin nanoparticles for the release of active compounds: a comparison, ChemSusChem. 13 (2020) 4759–4767, https://doi.org/10.1002/cssc.202001140.

[25] M. Lievonen, J.J. Valle-Delgado, M.-L. Mattinen, E.-L. Hult, K. Lintinen, M. A. Kostiainen, A. Paananen, G.R. Szilvay, H. Setälä, M. Österberg, A simple process for lignin nanoparticle preparation, Green Chem. 18 (2016) 1416–1422, https:// doi.org/10.1039/C5GC01436K.

[26] S. Beisl, P. Loidolt, A. Miltner, M. Harasek, A. Friedl, Production of micro- and nanoscale lignin from wheat straw using different precipitation setups, Molecules. 23 (2018) 633, https://doi.org/10.3390/molecules23030633.

[27] G. Colucci, A. Santamaria-Echart, S.C. Silva, L.G. Teixeira, A. Ribeiro, A. E. Rodrigues, M.F. Barreiro, Development of colloidal lignin particles through particle design strategies and screening of their Pickering stabilizing potential, Colloids Surf. A Physicochem. Eng. Asp. 666 (2023) 131287, https://doi.org/ 10.1016/j.colsurfa.2023.131287.

[28] W. Brand-Williams, M.E. Cuvelier, C. Berset, Use of a free radical method to evaluate antioxidant activity, LWT - Food Sci. Technol. 28 (1995) 25–30, https:// doi.org/10.1016/S0023-6438(95)80008-5.

[29] J. Domínguez-Robles, T. Tamminen, T. Liitiä, M.S. Peresin, A. Rodríguez, A.-S. Jääskeläinen, Aqueous acetone fractionation of kraft, organosolv and soda lignins, Int. J. Biol. Macromol. 106 (2018) 979–987, https://doi.org/10.1016/j. ijbiomac.2017.08.102.

[30] M. Ma, L. Dai, J. Xu, Z. Liu, Y. Ni, A simple and effective approach to fabricate lignin nanoparticles with tunable sizes based on lignin fractionation, Green Chem. 22 (2020) 2011–2017, https://doi.org/10.1039/D0GC00377H.

[31] O. Ajao, J. Jeaidi, M. Benali, A. Restrepo, N. El Mehdi, Y. Boumghar, Quantification and variability analysis of lignin optical properties for colour-dependent industrial applications, Molecules 23 (2018) 377, https://doi.org/10.3390/ molecules23020377.

[32] H. Zhang, S. Fu, Y. Chen, Basic understanding of the color distinction of lignin and the proper selection of lignin in color-depended utilizations, Int. J. Biol. Macromol. 147 (2020) 607–615, https://doi.org/10.1016/j.ijbiomac.2020.01.105.

[33] H. Zhang, F. Chen, X. Liu, S. Fu, Micromorphology influence on the color performance of lignin and its application in guiding the preparation of light-colored lignin sunscreen, ACS Sustain. Chem. Eng. 6 (2018) 12532–12540, https:// doi.org/10.1021/acssuschemeng.8b03464.

[34] I.V. Pylypchuk, M. Karlsson, P.A. Lindén, M.E. Lindström, T. Elder, O. Sevastyanova, M. Lawoko, Molecular understanding of the morphology and properties of lignin nanoparticles: unravelling the potential for tailored applications, Green Chem. 25 (2023) 4415–4428, https://doi.org/10.1039/ D3GC00703K.

[35] M.H. Sipponen, H. Lange, M. Ago, C. Crestini, Understanding lignin aggregation processes. a case study: budesonide entrapment and stimuli controlled release from lignin nanoparticles, ACS Sustain. Chem. Eng. 6 (2018) 9342–9351, https://doi. org/10.1021/acssuschemeng.8b01652.

[36] J.D. Zwilling, X. Jiang, F. Zambrano, R.A. Venditti, H. Jameel, O.D. Velev, O. J. Rojas, R. Gonzalez, Understanding lignin micro- and nanoparticle nucleation and growth in aqueous suspensions by solvent fractionation, Green Chem. 23 (2021) 1001–1012, https://doi.org/10.1039/D0GC03632C.

[37] J. Xu, R. Liu, L. Wang, X. Pan, J. Hemming, L. Dai, C. Xu, C. Si, Towards a deep understanding of the biomass fractionation in respect of lignin nanoparticle formation, Adv. Compos. Hybrid Mater. 6 (2023) 214, https://doi.org/10.1007/ s42114-023-00797-z.

[38] K. Hrůzová, K. Kolman, L. Matsakas, H. Nordberg, P. Christakopoulos, U. Rova, Characterization of organosolv lignin particles and their affinity to sulfide mineral

surfaces, ACS Appl. Nano Mater. 6 (2023) 17387–17396, https://doi.org/10.1021/acsanm.3c02069.

[39] J. Ou, S. Li, W. Li, C. Liu, J. Ren, F. Yue, Revealing the structural influence on lignin phenolation and its nanoparticle fabrication with tunable sizes, ACS Sustain. Chem. Eng. 10 (2022) 14845–14854, https://doi.org/10.1021/acssuschemeng.2c04701.

[40] Y. Yang, J. Xu, J. Zhou, X. Wang, Preparation, characterization and formation mechanism of size-controlled lignin nanoparticles, Int. J. Biol. Macromol. 217 (2022) 312–320, https://doi.org/10.1016/j.ijbiomac.2022.07.046.

[41] J. Tian, J. Chen, P. Wang, J. Guo, W. Zhu, M.R. Khan, Y. Jin, J. Song, O.J. Rojas, Interfacial activity and Pickering stabilization of kraft lignin particles obtained by solvent fractionation, Green Chem. 25 (2023) 3671–3679, https://doi.org/10.1039/D3GC00692A.

[42] I.V. Pylypchuk, A. Riazanova, M.E. Lindström, O. Sevastyanova, Structural and molecular-weight-dependency in the formation of lignin nanoparticles from fractionated soft- and hardwood lignins, Green Chem. 23 (2021) 3061–3072, https://doi.org/10.1039/D0GC04058D.

[43] M. Ago, S. Huan, M. Borghei, J. Raula, E.I. Kauppinen, O.J. Rojas, High-throughput synthesis of lignin particles (~30 nm to ~2 μm) via aerosol flow reactor: size fractionation and utilization in Pickering emulsions, ACS Appl. Mater. Interfaces. 8 (2016) 23302–23310, https://doi.org/10.1021/acsami.6b07900.

[44] M.H. Sipponen, M. Smyth, T. Leskinen, L.-S. Johansson, M. Österberg, All-lignin approach to prepare cationic colloidal lignin particles: stabilization of durable Pickering emulsions, Green Chem. 19 (2017) 5831–5840, https://doi.org/10.1039/C7GC02900D.

[45] M.R.V. Bertolo, L.B. Brenelli de Paiva, V.M. Nascimento, C.A. Gandin, M.O. Neto, C.E. Driemeier, S.C. Rabelo, Lignins from sugarcane bagasse: renewable source of nanoparticles as Pickering emulsions stabilizers for bioactive compounds encapsulation, Ind. Crops Prod. 140 (2019) 111591, https://doi.org/10.1016/j.indcrop.2019.111591.

[46] Z. Wang, Y. Wang, Tuning amphiphilicity of particles for controllable pickering emulsion, Materials (basel). 9 (2016) 903, https://doi.org/10.3390/ma9110903.

[47] S. Levine, B.D. Bowen, S.J. Partridge, Stabilization of emulsions by fine particles I. Partitioning of particles between continuous phase and oil/water interface, Colloids Surf. 38 (1989) 325–343, https://doi.org/10.1016/0166-6622(89)80271-9.

[48] A. Schröder, M.N. Corstens, K.K.H.Y. Ho, K. Schroën, C.C. Berton-Carabin, Pickering Emulsions, in: Emuls. Syst. Deliv. Food Act. Compd., Wiley, 2018, pp. 29–67. DOI: 10.1002/9781119247159.ch2.

[49] A. Ribeiro, J.C.B. Lopes, M.M. Dias, M.F. Barreiro, Pickering emulsions based in inorganic solid particles: from product development to food applications, Molecules. 28 (2023) 2504, https://doi.org/10.3390/molecules28062504.

[50] T. Dizhbite, G. Telysheva, V. Jurkjane, U. Viesturs, Characterization of the radical scavenging activity of lignins - natural antioxidants, Bioresour. Technol. 95 (2004) 309–317, https://doi.org/10.1016/j.biortech.2004.02.024.

[51] O. Gordobil, A. Oberemko, G. Saulis, V. Baublys, J. Labidi, In vitro cytotoxicity studies of industrial Eucalyptus kraft lignins on mouse hepatoma, melanoma and Chinese hamster ovary cells, Int. J. Biol. Macromol. 135 (2019) 353–361, https://doi.org/10.1016/j.ijbiomac.2019.05.111.

[52] Guo, Tian, Shen, Yang, Long, He, Song, Zhang, Zhu, Huang, Deng, Transparent Cellulose/Technical Lignin Composite Films for Advanced Packaging, Polymers (Basel). 11 (2019) 1455. DOI: 10.3390/polym11091455.

[53] X. Zhang, M. Yang, Q. Yuan, G. Cheng, Controlled preparation of corncob lignin nanoparticles and their size-dependent antioxidant properties: toward high value utilization of lignin, ACS Sustain. Chem. Eng. 7 (2019) 17166–17174, https://doi.org/10.1021/acssuschemeng.9b03535.

[54] S.R. Yearla, K. Padmasree, Preparation and characterisation of lignin nanoparticles: evaluation of their potential as antioxidants and UV protectants, J. Exp. Nanosci. 11 (2016) 289–302, https://doi.org/10.1080/17458080.2015.1055842.

[55] H. Trevisan, C.A. Rezende, Pure, stable and highly antioxidant lignin nanoparticles from elephant grass, Ind. Crops Prod. 145 (2020) 112105, https://doi.org/10.1016/j.indcrop.2020.112105.